

# Double-Flow GAN model for the reconstruction of perceived faces from brain activities

Zihao Wang<sup>1</sup>, Jing Zhao<sup>2,3</sup>, and Hui Zhang<sup>2,4,5</sup>

<sup>1</sup> School of Computer Science and Engineering, Beihang University, Beijing, China  
*zihao.wang@buaa.edu.cn*

<sup>2</sup> School of Engineering Medicine, Beihang University, Beijing, China

<sup>3</sup> School of Biological Science and Medical Engineering, Beihang University, Beijing, China

<sup>4</sup> Key Laboratory of Biomechanics and Mechanobiology, Ministry of Education, Beihang University, Beijing, China

<sup>5</sup> Key Laboratory of Big Data-Based Precision Medicine, Ministry of Industry and Information Technology of the People's Republic of China, Beihang University, Beijing, China  
*hui.zhang@buaa.edu.cn*

**Abstract.** Face plays an important role in human's visual perception, and reconstructing perceived faces from brain activities is challenging because of its difficulty in extracting high-level features and maintaining consistency of multiple face attributes, such as expression, identity, gender, etc. In this study, we proposed a novel reconstruction framework, which we called Double-Flow GAN, that can enhance the capability of discriminator and handle imbalances in images from certain domains that are too easy for generators. We also designed a pretraining process that uses features extracted from images as conditions for making it possible to pretrain the conditional reconstruction model from fMRI in a larger pure image dataset. Moreover, we developed a simple pretrained model to perform fMRI alignment to alleviate the problem of cross-subject reconstruction due to the variations of brain structure among different subjects. We conducted experiments by using our proposed method and state-of-the-art reconstruction models. Our results demonstrated that our method showed significant reconstruction performance, outperformed the previous reconstruction models, and exhibited a good generation ability.

**Keywords:** Perceived Face Reconstruction · Double-flow GAN · Brain decoding.

## 1 Introduction

Reconstruction perceived images from brain signals is a hot topic in brain decoding and a prospective part in brain-computer interface. Using functional Magnetic Resonance Imaging (fMRI), a non-invasive neuroimaging technique, researchers are able to measure the neural activities at each brain location across

the whole brain when performing particular visual tasks, and therefore makes perceptual image reconstruction from brain possible. So far, researchers have reconstructed various kinds of perceived images from fMRI brain activities, such as patterns [31], letters [22,28,6], scenes [30,1,23], natural objects [14,33,10].

Of these reconstructed natural objects, face is most special in human visual perception. Face plays a crucial role in our daily life. However, compared to common objects, reconstruction of perceived face faces is challenging. Firstly, compared to low-level visual features contained mostly in common objects, features that could represent face images are high-level [12], and are hard to extract and reconstruct. Secondly, face images contain many fine-grained features presented in details of images which are hard to reconstruct, such as identity, gender and expression. The minor pixelwise differences could cause major changes in the attributes of reconstructed faces. So it is difficult to preserve those attributes during reconstruction [14].

In this paper, we combined GAN [9] and transformer [34], and proposed a new algorithm framework to realize the perceived face reconstruction. The framework, which we termed Double-Flow GAN (DFGAN), have several improvements compared to the previous GAN-based reconstruction models. First, the discriminator of the GAN takes input from both positive and negative samples in a single forward process, which allows it to compare the two samples and ultimately decide which one is true. Second, due to the shortage of perceived face fMRI dataset, we train our framework in two stages. in the first stage, the DFGAN will be pretrained in a large dataset which only contains face images. In the second stage, the input features extracted from face selective brain regions of OFA, amygdala, STS, FFA and aIT will be aligned with face features and used as conditional in-puts to the GAN, and supervised by an enhanced discriminator to realize the face reconstruction.

## 2 Related Works

Many methods were used for perceived face reconstruction. Principle component analysis (PCA) was widely used in early years, for its ability to provide a compact representation of facial features by extracting a set of orthogonal basis vectors, known as eigenfaces [31]. Researchers could simplify the task of reconstructing face images with detailed attributes to the task of reconstructing low-dimensional feature vectors. As a result of it, combining PCA and basic supervised machine learning methods like support vector machine (SVM) and linear regression is also helpful [3,?]. Moreover, using extracted attributes or behavioral data to assist reconstruction can make a progress [14,25]. However, reconstruction based on feature extracted by PCA lose detailed information and the reconstructed images are very blurry.

In recent years, deep generative networks have shown great capability in image synthesis, and conditional generative networks like conditional generative adversarial networks (cGAN) provides a direct way for reconstructing face images from brain signals. The idea of generative adversarial networks (GAN)

is to train two neural networks, where the two networks engage in a competitive game that generator tries to generate images to fool the discriminator and discriminator tries to correctly classify real and fake samples. Works combining dimensionality reduction method with deep generative network have shown great abilities generating faces with high-resolution [4]. In addition, modifying the loss function of the GAN by adding attribute losses is also a good way to improve the consistency of reconstructed face attributes [14]. However, the discriminator in traditional GANs can only predict the truth or falsity of an image, whereas all faces are similar and differ only in details, which makes the generator's task easy and the discriminator's task difficult, which will harm the game between them and the reconstruction work. Moreover, the representation capability of CNN-based generators is not sufficient to generate high-resolution images. Finally, diffusion models (DM), which have been gaining attention and used in high-resolution natural-image reconstruction [2,30], were not applicable for perceived face reconstruction currently, because DMs focus on semantic contents reconstruction and are less of consistency, and minor changes in pixels of face images will cause changes in attributes.

Our proposed perceived face reconstruction framework DFGAN focused on the question of insufficient representation capability of cGAN and the imbalance between generator and discriminator. Our main contributions are as follows: 1) We proposed a novel GAN discriminator structure that can handle imbalances in images from certain domains that are too easy for generators. 2) We designed a pretraining process using features extracted from images as conditions that can be used in domains where neural data is lacking.

### 3 Method

#### 3.1 fMRI Alignment

Because the brain structure differs among people, there is a big difference between fMRI signals collected from different individuals. Therefore, it's hard to synthesis faces directly through fMRI data collected from different people. Here, we padded the data to the same size and tried to learn a linear model that could project fMRI to the feature of face images, which we called fMRI alignment.

As shown in Fig 1 A, we used a pretrained VGG Face to extract the feature of image, and learned a linear model to map the fMRI data to the feature, with MSE loss as the loss function.

#### 3.2 Transformer Generator

Generating high-resolution images using Transformers are computationally demanding due to the large number of pixels involved. To reduce the large computational complexity of the global attention, we utilized Swin Transformer [20], which processes the entire image into several separate non-overlapping patches called "windows." The Swin Transformer consists of several stages, each composed of a set of Swin Transformer blocks. Each block contains two sub-layers:

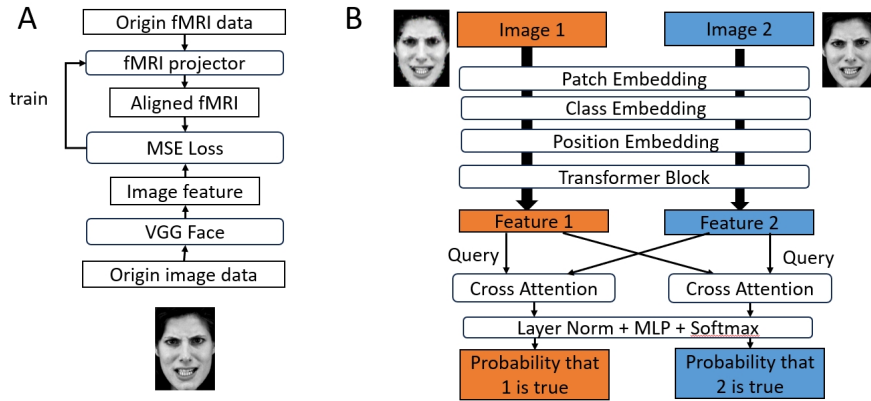


**Fig. 1.** A Training process of fMRI projector. B Architecture of Double-flow Transformer Discriminator, which uses cross attention to combine the information of two images.

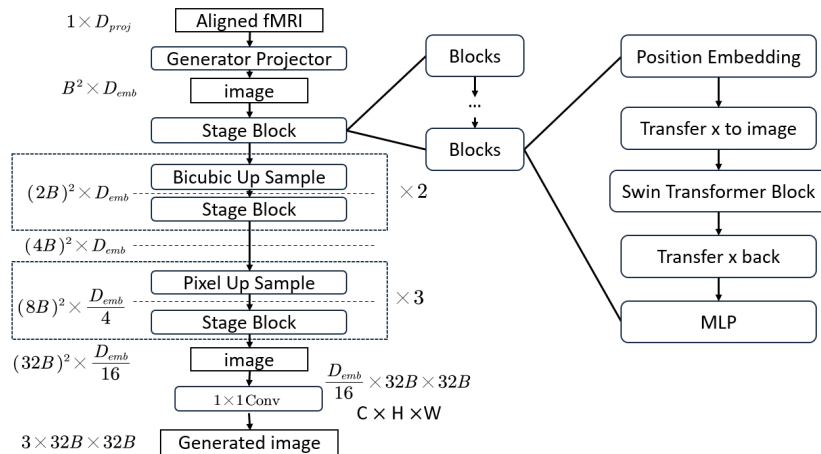


**Fig. 2.** The architecture of our generator based on Swin Transformer.

a shifted window-based self-attention mechanism and a feed-forward neural network. The shifted window-based self-attention mechanism enables the model to capture long-range dependencies within the image by shifting the windows and attending to neighboring windows.

Swin Transformer has shown great power in computer vision tasks such as classification and segmentation, and we propose to use Swin Transformer in the conditional generation task. Given condition  $z$ , which is the projected fMRI data in the latent space, our model will project the fMRI data further into an embedding  $x = \tau_\theta(z) \in \mathbf{R}^{B^2 \times D_{emb}}$ , where  $B$  representing the bottom-width and  $D_{emb}$  represents the dimension of embedding. So,  $x$  could be seen as an  $B \times B$  image with  $D_{emb}$  channels and we can use  $x$  as the input of Swin Transformer. Considering both high-resolution image generation and computation cost, we use bicubic up sample at early stage and pixel shuffle at latter stage, with stage blocks using Swin Transformer between them. The detailed generative model is showed in Fig 2.

### 3.3 Double-flow Transformer Discriminator

Facial images have similar features in general, such as round facial contours, two eyes, one mouth, etc. The similarities between all training data will make it easy for generator to generate realistic images which are enough to mislead the discriminator. Even the attributes of generated faces may not accurate, discriminator can only admit that they are true. The imbalance between them will let the further optimization in generator harder. Also, the consistency of the reconstructed images is important when generating them from fMRI that a person can only perceive single face at one time. In order to drive the generator to reconstruct images with high quality and consistency, we introduced two methods to make the discriminator powerful.

First, we improved the architecture of discriminator. Unlike previous discriminator, which only takes one image as input, we introduced Double-flow Transformer Discriminator, which takes both real images and fake images in a single process. As shown in Fig. 1 B, real-fake image pairs are input into the model, and the output of model is a pair of numbers between 0 to 1 that are added up to one, representing the probability that image 1 or 2 is true. In the model, we use Cross-Attention [8] method to let the model “compare” the two images, so the model only needs to decide which image is true, instead of judging whether an image is true only seeing the image itself.

Second, like the method in [14], we modified the final layer of the discriminator, and increased the task for discriminator that it could not only justify the image is real or not, but also predict the face’s identity, gender and expression, irrespectively. As a result, we could further modify the loss function, and the loss function of the discriminator is defined as:

$$\begin{aligned} \max_D L_{GAN}^D &= E_{x \sim P_x(x)} [\log D(x)] + E_{z \sim P_z(z)} [\log(1 - D(G(z)))] \\ &\quad - \alpha \times (L_{BCE}(t_{attr}, D_{attr}(x)) + D(G(z)) \times L_{BCE}(t_{attr}, D_{attr}(G(z)))) \end{aligned} \quad (1)$$

where  $x$  is the real face images,  $z$  is the aligned latent of fMRI,  $t_{attr}$  is a concatenation of features of face identity, expression and gender,  $L_{BCE}$  is the binary cross-entropy loss and  $D(x)$  is the possibility that discriminator predicted the image real or fake. Compared with the loss function proposed in [14], we added a factor of confidence level to the attribute loss, with the insight that the discriminator has less responsible for the predicted attributes of the image which is predicted fake.

According to the discriminator loss, the generator loss has the same structure, which is defined as:

$$\begin{aligned} \min_G L_{GAN}^G = & [\log(1 - D(G(z)))] + \lambda L_{MAE}(G(z), x) \\ & + \alpha D(G(z)) \times L_{BCE}(t_{attr}, D_{attr}(G(z))) \end{aligned} \quad (2)$$

where  $L_{MAE}$  is the MAE loss and the other annotations are the same as the equation shown above. Compared with the loss function proposed in [14], we added an attribute loss for the generator with insight that the generator should have responsible for attributes of the generated images that are sufficient to confuse the discriminator.

### 3.4 The training Pipeline

The whole training process are divided into three steps, 1) training the fMRI projector; 2) pretraining the GAN in a large face dataset; 3) finetuning the GAN in the limited fMRI-face pair dataset. As the first step is fully described, we are going to talk about the other two steps in details.

In the second step, we trained the generator of GAN with a large dataset of human faces, in order to let the generator get familiar with the structure of human faces. Because the fMRI data have aligned with feature of image, we use the feature extracted by VGG Face as the condition of the generator. It worth mentioning that we used the raw discriminator that only predicts whether the image is true or not, in order to reduce the usage of computational resources in such a large dataset.

In the third step, we took the aligned fMRI data as the condition input of GAN, using the loss function above to force the generator, which already have the ability to generate face images, to generate image with consistency of the attributes.

## 4 Experiments

### 4.1 Dataset, Experimental Setup and Baseline

We used the CelebA dataset for the pretrain part of the model [14]. The dataset contains 30,000 of face images. We only use the face images in the dataset, and each image was resized to  $224 \times 224$  to meet the requirement of input of VGG Face. Also, the images were resized to  $128 \times 128$  before put into the discriminator in order to meet the shape of reconstructed images.

Moreover, we used the fMRI-face pair dataset introduced in the previous paper [8]. Briefly, the dataset contains 2,800 pairs of fMRI images acquired from the OFA, amygdala, STS, FFA, and aIT brain regions of 2 individuals, each containing 1,400 pairs divided into 1,260 pairs for training and 140 pairs for evaluation. We used the fMRI data which has been processed by the MTDLN introduced in the same paper, which mapped the original to a feature space under supervision of the identity, gender and expression attribute. We used the processed fMRI as the input of fMRI projector introduced in 3.1 and utilized the attributes as attribute loss in 3.3. More details about the dataset is provided in the original paper.

We implemented our model in PyTorch with one NVIDIA GeForce RTX 4090 GPU which has 25GB of memory. Our model is trained using the Adam optimizer with a learning rate of 2e-4, for 200 epochs in stage 1 and 500 epochs in stage 2. The parameters and is empirically set to 10 and 0.01. All other hyper-parameters are retrained using their default settings.

We compared our model to the method used in the original paper [14]. The baseline model is mcGAN, and used a simpler loss function:

$$\begin{aligned} \max_D L_{GAN}^D &= E_{x \sim P_d(x)}[\log D(x)] + E_{z \sim P_z(z)}[\log(1 - D(G(z)))] \\ &- \lambda_D \{L_{BCE}(t_{id}, D_{\text{class}_{id}}(x)) + L_{BCE}(t_{id}, D_{\text{class}_{id}}(G(z))) \\ &+ L_{BCE}(t_{\text{exp}}, D_{\text{class}_{\text{exp}}}(x)) + L_{BCE}(t_{\text{exp}}, D_{\text{class}_{\text{exp}}}(G(z))) \\ &+ L_{BCE}(t_{\text{gen}}, D_{\text{class}_{\text{gen}}}(x)) + L_{BCE}(t_{\text{gen}}, D_{\text{class}_{\text{gen}}}(G(z)))\} \end{aligned} \quad (3)$$

$$\min_G L_{GAN}^G = E_{z \sim P_z(z)}[\log(1 - D(G(z)))] + \lambda_G L_{MAE}(G(z), x) \quad (4)$$

where notations are the same as the origin paper.

## 4.2 Quantitative Results and Ablation Experiments

**Table 1.** Quantitative results on dataset using different models, in terms of SSIM, MSE and Attribute error. The attribute error is computed from a pre-trained ResNet 50 that can predict the attribute scores of the real image, where the loss is between the predicted attribute scores of the generated image and the real attributes. The best results are marked in red. All fMRI data (contains baseline) are projected. T represents Transformer and dfD represents our double-flow Discriminator.

Model	MSE	SSIM	Attribute error
Baseline (mcGAN)	0.046	0.578	0.932
CNNG+TD	0.027	0.689	0.899
CNNG+dfD	0.028	0.669	0.907
TG+TD	0.027	0.695	0.900
proposed model (dfGAN)	0.025	0.695	0.899



**Fig. 3.** Samples of the generated images.

We tested our proposed model, baseline model on the dataset and removed /replaced some part of proposed model. Fig. 3 shows the reconstruction effect of different models on the first 8 images in the test set and Table 1 reports the average SSIM , MSE scores and attribute error. The results show that improvements can be obtained using either the Transformer-based generator or the discriminator. Especially, our proposed discriminator is better than Transformer discriminator when using Transformer generator, but weaker than it when using CNN generator. We think this might be because our enhanced discriminator achieved a good balance with the Transformer generator but was too strong for the CNN generator.

**Table 2.** Quantitative results of ablation experiments, in terms of SSIM, MSE and attribute error. The base model is dfGAN. The best results are marked in red.

align	loss function	pretrain	MSE	SSIM	Attribute error
yes	our	yes	0.025	0.695	0.899
no	our	yes	9.235	0.259	9.891
yes	past	yes	0.027	0.679	0.910
yes	origin	yes	0.031	0.667	0.904
yes	our	no	0.309	0.608	0.926

Table 2 shows the results of ablation experiments, which highlights the significance of fMRI alignment, as the Transformer generator is unable to reconstruct meaningful images from fMRI data that is not aligned with the corresponding image.

### 4.3 Sensitivity Analysis

In order to further examine how the hyper-parameters influence reconstruction performance, we tested our model on different  $\alpha$  and  $\lambda$ . According to Fig. 4 A, when  $\alpha$  is 0.01, the SSIM score meets the top and the misjudge score are in the middle between 0 and 1, which aligns with the insight that GAN performs best when the capability of generator and discriminator evenly matched. The Fig. 4 B shows that generator and discriminator will keep competitive when  $\alpha$  is 0.01. Moreover, all above shows that the performance holds up well with three orders of magnitude of variation in the hyper-parameters.

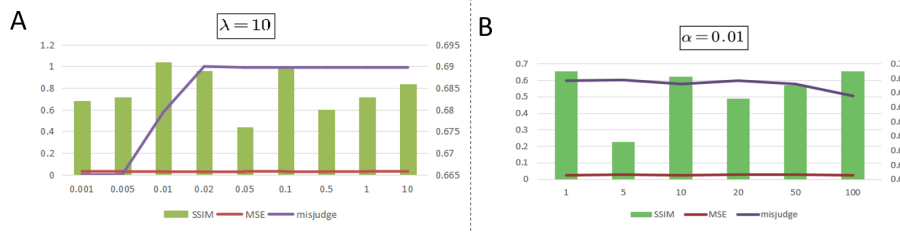


**Fig. 4.** Results of sensitivity analysis.  $\alpha$  is the horizontal coordinate of A, and  $\lambda$  is the horizontal coordinate of B. For both images, misjudge and MSE are left vertical coordinate, SSIM is right vertical coordinate. The score of misjudge represents what percentage of false images the discriminator will determine as true.

### 4.4 Generalization Capability

Due to the significant variation in fMRI data extracted from different individuals, there is a challenge in achieving generalization capability with reconstruction models. In order to address this issue, we tested to determine if the reconstruction model could accurately reconstruct perceived images for new individuals. Our dataset contains fMRI data from two person. We used data from one person for training, and evaluated the model’s performance on the fMRI data from the other person for testing. Table 3 reports the MSE and SSIM scores of the model trained on one individual and tested on the other one.

## 5 Conclusion and Discussion

In this paper, we presented a training pipeline for cross-modal generation like reconstruction images from fMRI where image-neural data pairs are lacking but

**Table 3.** Quantitative results of the Inter-subject experiments

train	test	MSE	SSIM	Attribute error
1	2	0.029	0.663	0.911
2	1	0.029	0.639	0.906
1	1	0.027	0.677	0.908
2	2	0.028	0.647	0.906

data from image domain is sufficient. Also, we proposed a novel reconstruction framework called DFGAN. The proposed DFGAN mitigates the imbalance of generating only one category of images that is too easy for the generator and too difficult for the discriminator. We also designed a pretraining process using features extracted from images as conditions that can be used in domains where neural data is lacking. Our method achieves improvements on performance and robust in the current dataset, and shows great generalization capability.

## References

1. Beliy, R., Gaziv, G., Hoogi, A., Strappini, F., Golan, T., Irani, M.: From voxels to pixels and back: Self-supervision in natural-image reconstruction from fmri. *Advances in Neural Information Processing Systems* **32** (2019)
2. Chen, Z., Qing, J., Xiang, T., Yue, W.L., Zhou, J.H.: Seeing beyond the brain: Conditional diffusion model with sparse masked modeling for vision decoding. In: *Proceedings of the IEEE/CVF Conference on Computer Vision and Pattern Recognition*. pp. 22710–22720 (2023)
3. Cowen, A.S., Chun, M.M., Kuhl, B.A.: Neural portraits of perception: reconstructing face images from evoked brain activity. *Neuroimage* **94**, 12–22 (2014)
4. Dado, T., Güçlütürk, Y., Ambrogioni, L., Ras, G., Bosch, S., van Gerven, M., Güçlü, U.: Hyperrealistic neural decoding for reconstructing faces from fmri activations via the gan latent space. *Scientific reports* **12**(1), 141 (2022)
5. Du, C., Du, C., He, H.: Sharing deep generative representation for perceived image reconstruction from human brain activity. In: *2017 International Joint Conference on Neural Networks (IJCNN)*. pp. 1049–1056. IEEE (2017)
6. Du, C., Du, C., Huang, L., He, H.: Reconstructing perceived images from human brain activities with bayesian deep multiview learning. *IEEE transactions on neural networks and learning systems* **30**(8), 2310–2323 (2018)
7. Du, C., Du, C., Huang, L., Wang, H., He, H.: Structured neural decoding with multitask transfer learning of deep neural network representations. *IEEE Transactions on Neural Networks and Learning Systems* **33**(2), 600–614 (2020)
8. Gheini, M., Ren, X., May, J.: Cross-attention is all you need: Adapting pretrained transformers for machine translation. *arXiv preprint arXiv:2104.08771* (2021)
9. Goodfellow, I., Pouget-Abadie, J., Mirza, M., Xu, B., Warde-Farley, D., Ozair, S., Courville, A., Bengio, Y.: Generative adversarial nets. *Advances in neural information processing systems* **27** (2014)
10. Güçlütürk, Y., Güçlü, U., Seeliger, K., Bosch, S., van Lier, R., van Gerven, M.A.: Reconstructing perceived faces from brain activations with deep adversarial neural decoding. *Advances in neural information processing systems* **30** (2017)

11. Heeger, D.J., Ress, D.: What does fmri tell us about neuronal activity? *Nature reviews neuroscience* **3**(2), 142–151 (2002)
12. Hershler, O., Hochstein, S.: At first sight: A high-level pop out effect for faces. *Vision research* **45**(13), 1707–1724 (2005)
13. Horikawa, T., Cowen, A.S., Keltner, D., Kamitani, Y.: The neural representation of visually evoked emotion is high-dimensional, categorical, and distributed across transmodal brain regions. *Iscience* **23**(5), 101060 (2020)
14. Hou, X., Zhao, J., Zhang, H.: Reconstruction of perceived face images from brain activities based on multi-attribute constraints. *Frontiers in Neuroscience* **16**, 1015752 (2022)
15. Huth, A.G., Lee, T., Nishimoto, S., Bilenko, N.Y., Vu, A.T., Gallant, J.L.: Decoding the semantic content of natural movies from human brain activity. *Frontiers in systems neuroscience* **10**, 81 (2016)
16. Kay, K.N., Naselaris, T., Prenger, R.J., Gallant, J.L.: Identifying natural images from human brain activity. *Nature* **452**(7185), 352–355 (2008)
17. Koide-Majima, N., Nakai, T., Nishimoto, S.: Distinct dimensions of emotion in the human brain and their representation on the cortical surface. *NeuroImage* **222**, 117258 (2020)
18. Lee, H., Kuhl, B.A.: Reconstructing perceived and retrieved faces from activity patterns in lateral parietal cortex. *Journal of Neuroscience* **36**(22), 6069–6082 (2016)
19. Lin, Y., Li, J., Wang, H.: Dcnn-gan: Reconstructing realistic image from fmri. In: 2019 16th International Conference on Machine Vision Applications (MVA). pp. 1–6. IEEE (2019)
20. Liu, Z., Lin, Y., Cao, Y., Hu, H., Wei, Y., Zhang, Z., Lin, S., Guo, B.: Swin transformer: Hierarchical vision transformer using shifted windows. In: Proceedings of the IEEE/CVF international conference on computer vision. pp. 10012–10022 (2021)
21. Liu, Z., Luo, P., Wang, X., Tang, X.: Deep learning face attributes in the wild. In: Proceedings of the IEEE international conference on computer vision. pp. 3730–3738 (2015)
22. Miyawaki, Y., Uchida, H., Yamashita, O., Sato, M.a., Morito, Y., Tanabe, H.C., Sadato, N., Kamitani, Y.: Visual image reconstruction from human brain activity using a combination of multiscale local image decoders. *Neuron* **60**(5), 915–929 (2008)
23. Mozafari, M., Reddy, L., VanRullen, R.: Reconstructing natural scenes from fmri patterns using bigbigan. In: 2020 International joint conference on neural networks (IJCNN). pp. 1–8. IEEE (2020)
24. Naselaris, T., Prenger, R.J., Kay, K.N., Oliver, M., Gallant, J.L.: Bayesian reconstruction of natural images from human brain activity. *Neuron* **63**(6), 902–915 (2009)
25. Nestor, A., Plaut, D.C., Behrmann, M.: Feature-based face representations and image reconstruction from behavioral and neural data. *Proceedings of the National Academy of Sciences* **113**(2), 416–421 (2016)
26. Nishida, S., Nishimoto, S.: Decoding naturalistic experiences from human brain activity via distributed representations of words. *Neuroimage* **180**, 232–242 (2018)
27. Rombach, R., Blattmann, A., Lorenz, D., Esser, P., Ommer, B.: High-resolution image synthesis with latent diffusion models. In: Proceedings of the IEEE/CVF conference on computer vision and pattern recognition. pp. 10684–10695 (2022)
28. Schoenmakers, S., Barth, M., Heskes, T., Van Gerven, M.: Linear reconstruction of perceived images from human brain activity. *NeuroImage* **83**, 951–961 (2013)

29. St-Yves, G., Naselaris, T.: Generative adversarial networks conditioned on brain activity reconstruct seen images. In: 2018 IEEE international conference on systems, man, and cybernetics (SMC). pp. 1054–1061. IEEE (2018)
30. Takagi, Y., Nishimoto, S.: High-resolution image reconstruction with latent diffusion models from human brain activity. In: Proceedings of the IEEE/CVF Conference on Computer Vision and Pattern Recognition. pp. 14453–14463 (2023)
31. Thirion, B., Duchesnay, E., Hubbard, E., Dubois, J., Poline, J.B., Lebihan, D., Dehaene, S.: Inverse retinotopy: inferring the visual content of images from brain activation patterns. *Neuroimage* **33**(4), 1104–1116 (2006)
32. Uğurbil, K., Xu, J., Auerbach, E.J., Moeller, S., Vu, A.T., Duarte-Carvajalino, J.M., Lenglet, C., Wu, X., Schmitter, S., Van de Moortele, P.F., et al.: Pushing spatial and temporal resolution for functional and diffusion mri in the human connectome project. *Neuroimage* **80**, 80–104 (2013)
33. VanRullen, R., Reddy, L.: Reconstructing faces from fmri patterns using deep generative neural networks. *Communications biology* **2**(1), 193 (2019)
34. Vaswani, A., Shazeer, N., Parmar, N., Uszkoreit, J., Jones, L., Gomez, A.N., Kaiser, L., Polosukhin, I.: Attention is all you need. *Advances in neural information processing systems* **30** (2017)